The American Journal of Pathology, Vol. 171, No. 6, December 2007

DOI: 10.2353/ajpath.2007.070198

Gastrointestinal, Hepatobiliary and Pancreatic Pathology

Homeostatic Control of the Crypt-Villus Axis by the Bacterial Enterotoxin Receptor Guanylyl Cyclase C Restricts the Proliferating Compartment in Intestine

Peng Li,* Jieru E. Lin,* Inna Chervoneva,† Stephanie Schulz,* Scott A. Waldman,* and Giovanni M. Pitari*

From the Divisions of Clinical Pharmacology, and Biostatistics,† Department of Pharmacology and Experimental Therapeutics, Thomas Jefferson University, Philadelphia, Pennsylvania*

Guanylyl cyclase C (GC-C), the receptor for diarrheagenic enterotoxins and the paracrine ligands guanylin and uroguanylin, regulates intestinal secretion. Beyond volume homeostasis, its importance in modulating cancer cell proliferation and its uniform dysregulation early in colon carcinogenesis, reflecting loss of ligand expression, suggests a role for GC-C in organizing the crypt-villus axis. Here, eliminating GC-C expression in mice increased crypt length along a decreasing rostral-caudal gradient by disrupting component homeostatic processes. Crypt expansion reflected hyperplasia of the proliferating compartment with reciprocal increases in rapidly cycling progenitor cells and reductions in differentiated cells of the secretory lineage, including Paneth and goblet cells, but not enteroendocrine cells. GC-C signaling regulated proliferation by restricting the cell cycle at the G_1/S transition. Moreover, crypt expansion in GC-C$^{-/-}$ mice was associated with adaptive increases in cell migration and apoptosis. Reciprocal alterations in proliferation and differentiation resulting in expansion associated with adaptive responses in migration and apoptosis suggest that GC-C coordinates component processes maintaining homeostasis of the crypt progenitor compartment. In the context of uniform loss of GC-C signaling during tumorigenesis, dysregulation of those homeostatic processes may contribute to mechanisms underlying colon cancer. *(Am J Pathol 2007, 171:1847–1858; DOI: 10.2353/ajpath.2007.070198)*

The intestinal epithelium undergoes homeostatic cycles of proliferation, migration, differentiation, and apoptosis entrained by the regenerative activity of multipotent stem cells.[1,2] Although mechanisms coordinating homeostasis are incompletely defined, they maintain the intestinal mucosa integrity despite constant exposure to environmental insults. In that context, specialized functions such as digestion and absorption of nutrients are accomplished by the action of a heterogeneous monolayer of columnar epithelial cells along the crypt-villus (small intestine) and crypt-surface (colon) axes.[1] Slowly-cycling stem cells located near crypt bottoms produce rapidly-cycling progenitor cells in mid-crypts, which initiate programs of lineage commitment through complex regulatory signaling,[2] forming mature absorptive cells or enterocytes and secretory cells, including mucus-producing goblet cells and peptide-producing enteroendocrine and Paneth cells.[1,3] Mature epithelial cells are replaced as they migrate toward the lumen side of the mucosa where they undergo apoptosis and shedding.[3]

An imbalance in component processes underlying homeostasis may be one fundamental mechanism contributing to the development of colon cancer,[4] the second leading cause of cancer-related mortality in developed countries.[5] Thus, targeted inactivation of p21,[6] which regulates cell cycle progression and differentiation, promotes APC mutation-dependent tumor formation by increasing proliferation and decreasing apoptosis and differentiation in intestine. Deletion of Muc2 in differentiated cells induces colorectal cancer by increasing proliferation and migration and decreasing apoptosis.[7] Conversely, crypt hyperplasia associated with disrupted dif-

Supported by the National Institutes of Health (grants CA75123 and CA95026 to S.A.W.), Targeted Diagnostic and Therapeutics Inc. (to S.A.W.), and the Pennsylvania Department of Health (to G.M.P.).

Accepted for publication August 23, 2007.

The Pennsylvania Department of Health specifically disclaims responsibility for any analyses, interpretations, or conclusions. S.A.W. is the Samuel M.V. Hamilton Endowed Professor.

S.A.W. and G.M.P. contributed equally to this study.

Address reprint requests to Giovanni Mario Pitari, M.D., Ph.D., Department of Pharmacology and Experimental Therapeutics, Thomas Jefferson University, 1100 Walnut St./MOB 810, Philadelphia, PA 19107; or Scott A. Waldman, M.D., Ph.D., Department of Pharmacology and Experimental Therapeutics, Thomas Jefferson University, 132 South 10th St., 1170 Main, Philadelphia, PA 19107. E-mail: giovanni.pitari@jefferson.edu and scott.waldman@jefferson.edu.

ferentiation, without changes in proliferation or apoptosis, promotes intestinal tumorigenesis in mice exhibiting loss of imprinting of the insulin-like growth factor II gene.[8]

Guanylyl cyclase C (GC-C), the receptor for bacterial diarrheagenic heat-stable enterotoxins (STs) and the endogenous ligands guanylin and uroguanylin, is the primary endogenous source of cyclic guanosine 3′,5′ monophosphate (cGMP) in intestinal epithelial cells.[9,10] Heretofore, GC-C and its downstream effector cGMP were considered principal regulators of intestinal fluid homeostasis. Intriguingly, GC-C has recently emerged as a key regulator of colon cancer cell dynamics. GC-C signaling through cyclic nucleotide gated channel disrupts tumor cell cycle progression and proliferation.[11–13] In close agreement, induction of cGMP-dependent mechanisms produces enduring colon cancer cytostasis.[13] Further, treatment of *Apc*$^{Min/+}$ mice with oral uroguanylin suppresses intestinal tumor formation.[14] However, although cGMP coordinates proliferation, differentiation, and apoptosis in many cell systems,[15,16] a role for GC-C in regulating component processes underlying crypt-villus homeostasis remains elusive. That GC-C might regulate crypt-villus homeostasis is supported by the near-uniform loss of guanylin and uroguanylin expression early in intestinal tumorigenesis.[17–19] Indeed, eliminating guanylin expression in mice induces expansion of the proliferating crypt compartment in colon,[20] although this effect is ostensibly not mimicked by elimination of GC-C expression.[21]

These observations suggest that GC-C and its ligands may function as a paracrine system regulating component processes underlying intestinal mucosa homeostasis. Moreover, GC-C signaling may represent a novel homeostatic mechanism whose dysregulation through loss of ligand expression contributes to colon carcinogenesis. The present studies explored the role of GC-C in coordinating processes organizing the crypt-villus axis, including proliferation, cell cycle, migration, differentiation, and apoptosis.

Materials and Methods

Cell Culture, Mice, and Reagents

NCM460 cells,[22] which express GC-C mRNA (Figure 1A) and functional GC-C protein (Figure 1, B–E), and their proprietary M3:10 medium were from In Cell (San Anto-

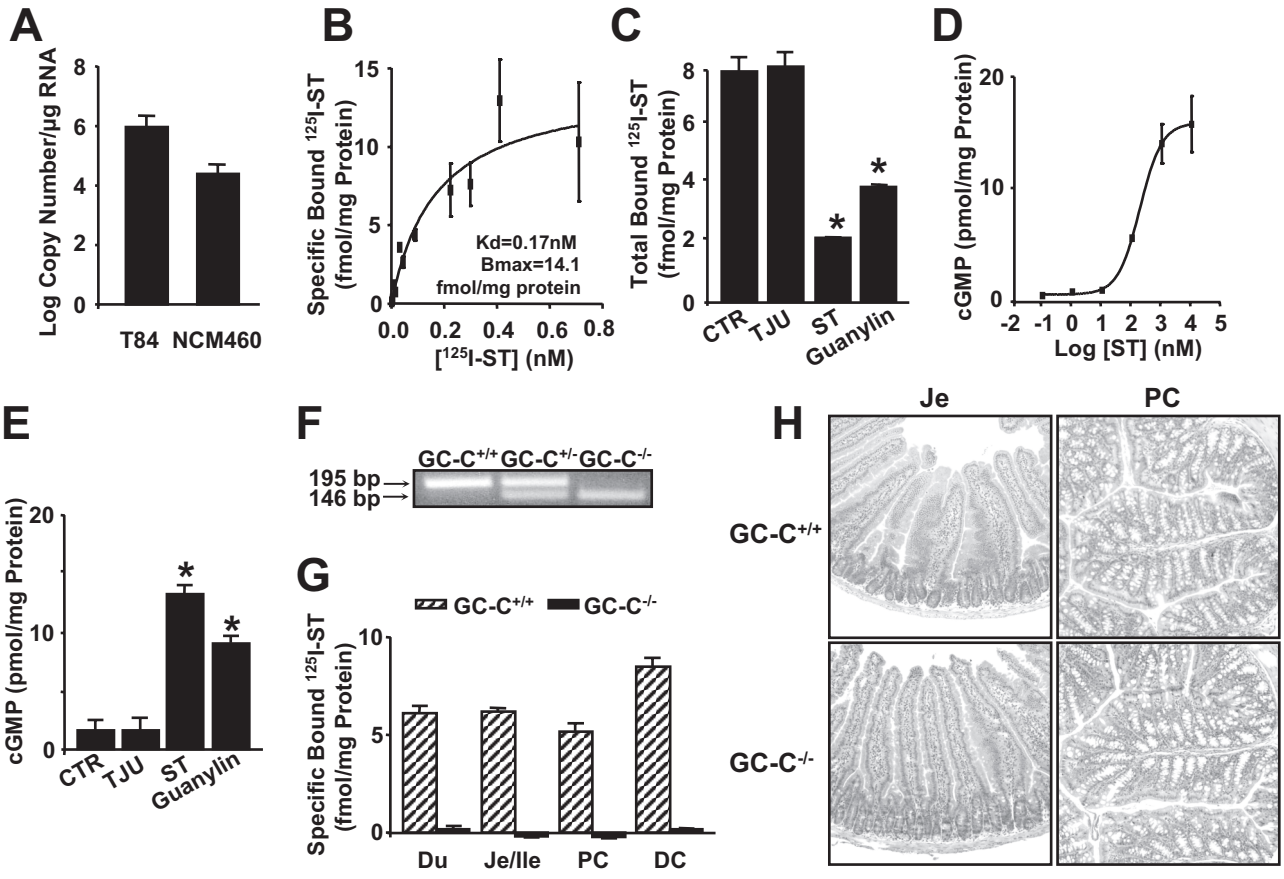

Figure 1. GC-C expression in NCM460 cells and GC-C$^{-/-}$ mice. **A:** GC-C mRNA is present in normal NCM460 colonocytes and T84 colon carcinoma cells (positive control) as assessed by RT-PCR (1 μg RNA of sample/reaction). **B:** Dose response of ^{125}I-ST binding to NCM460 membranes (cold competitor, 1 μmol/L ST). kDa, ST binding affinity, Bmax, maximum number of ST binding sites. **C:** Total binding of ^{125}I-ST to NCM460 membranes in the presence of the vehicle (CTR, control) or the inactive ST analog TJU 1-103 (TJU, 1 μmol/L), ST (1 μmol/L), or guanylin (1 μmol/L) as cold competitors. In NCM460 cells, ST induces cGMP accumulation in a dose-dependent manner (**D**), an effect mimicked by guanylin (1 μmol/L) but not the vehicle (CTR, control) or the inactive analog TJU 1-103 (TJU, 1 μmol/L) (**E**; ST, 1 μmol/L). **F:** PCR on DNA extracts yielded the expected 195-bp (GC-C$^{+/+}$) and 146-bp (GC-C$^{-/-}$) amplicons. **G:** Specific ^{125}I-ST binding (cold competitor, 1 μmol/L ST) to intestinal mucosa membranes isolated from GC-C$^{+/+}$ (hatched columns) and GC-C$^{-/-}$ (black columns) mice. **H:** H&E staining of representative GC-C$^{+/+}$ and GC-C$^{-/-}$ mouse intestinal sections. Du, duodenum; Je/Ile, jejunum and ileum; PC, proximal colon; and DC, distal colon. *$P < 0.05$, two-tailed *t*-test. Original magnifications, ×100.

nio, TX). T84 human colon carcinoma cells, used as a positive control for GC-C expression,[23] were from American Type Culture Collection (Manassas, VA).

GC-C$^{-/-}$ mice, generated by neomycin-resistant gene insertion,[24] were genotyped after polymerase chain reaction (PCR) of genomic DNA isolated from tails (GC-C forward primer, 5′-AGGTCATGACGTCACTGCTGGGCC-3′; GC-C reverse primer, 5′-TGTCCAGTCCTTCCTCCA-CAG-3′; neomycin reverse primer, 5′-GGTGGGCTCTAT-GGCTTC-3′) (Figure 1F) and exhibited loss of GC-C ligand binding in their intestine (Figure 1G). GC-C$^{-/-}$ mice (I-129 background) were backcrossed with a C57BL/6 strain for seven or more generations, and GC-C$^{-/-}$ and GC-C$^{+/+}$ littermates (males, 3 months old) were analyzed. Animals were maintained in a controlled environment (20°C, 12-hour dark/light cycle) with free access to food and water. For cell migration, three GC-C$^{-/-}$ and three GC-C$^{+/+}$ mice per time point (2, 24, and 48 hours) were analyzed. These animals (nine GC-C$^{-/-}$ and nine GC-C$^{+/+}$ mice) were also used for examining other morphometric or cytodynamic parameters. Two additional cohorts of six mice per genotype were used for calculations of cell cycle times. Finally, two additional cohorts of five mice per genotype were used for immunoblot analyses. Reagents used included native ST and the inactive analog ST(5–17)Ala,^{9,17}Cys(Acm),^{5,10}6-14 disulfide (TJU 1-103) (Bachem, San Carlos, CA); [*methyl*-^{3}H]thymidine (Amersham, Piscataway, NJ), and 3-isobutyl-1-methylxanthine, guanylin, 8-br-cGMP (Sigma, St. Louis, MO).

Crypt Depth

Mouse intestines were isolated, cleaned, and divided into five segments: duodenum (the rostral, 5-cm-long small intestinal segment from the pyloric sphincter), jejunum (the rostral half of small intestine from the duodenum to the ileal-cecal junction), ileum (the caudal half of small intestine from the duodenum to the ileal-cecal junction), and proximal (the rostral half) and distal (the caudal half) colon (from the cecal-colonic junction to the anal sphincter). Intestinal samples, spanning 1 cm (small intestine) or 0.5 cm (colon) from the center of each segment, were fixed overnight (10% formalin), embedded in paraffin, sectioned (5 μm), and mounted (5 to 20 sections/slide) for hematoxylin and eosin (H&E) staining. Digital images were captured with a light microscope attached to a computer and recorded using Adobe Photoshop. Crypt length was measured (in $\geq$10 crypts/intestinal segment/mouse) as the distance from the bottom to the opening of crypt with intact columnar epithelia using the NIH Image J analysis software.

In Vivo *Cell Proliferation, Cell Differentiation, and Cell Death*

Intestinal sections were deparaffinized and rehydrated with sequential washes of xylene, ethanol, and water, followed by heat-induced epitope retrieval (10 mmol/L citrate buffer, ph 6.0). Sections were incubated with primary antibodies (overnight, 4°C), followed by secondary antibodies and diaminobenzidine substrate (avidin-biotin kit; Vector Laboratories, Burlingame, CA). Stained cells were quantified (in 5 to 15 crypt-villus units/intestinal segment/mouse) using NIH Image J software. Proliferating cells were stained with the proliferating cell nuclear antigen (PCNA) immunohistochemistry (IHC) kit (Zymed, South San Francisco, CA) or the rat anti-mouse Ki-67 antibody (1:50 dilution; DAKO Cytomation, Carpinteria, CA). PCNA- and Ki-67-labeling indices were calculated by normalizing the number of PCNA- or Ki-67-positive cells to the total cell number in respective crypts. Paneth cells, enterocytes, and enteroendocrine cells were stained with rabbit anti-human/mouse lysozyme antibody (ready-to-use, DAKO Cytomation), goat anti-villin antibody [Villin(C-19), 1:25 dilution; Santa Cruz Biotechnology, Santa Cruz, CA], and rabbit anti-chromogranin A antibody (1:200 dilution, Zymed), respectively. Goblet cells were quantified using Alcian blue staining of mucin[7] with fast nuclear red counterstaining. Finally, cell death was quantified by terminal deoxynucleotidyl transferase-mediated dNTP-biotin nick-end labeling (TUNEL) using the TACSXL blue label *in situ* apoptosis detection kit (Trevigen, Gaithersburg, MD).

In Vivo *Cell Cycle and Cell Migration*

Crypt cell cycles were examined by cumulative BrdU (15 mg/kg) injections (at 4- to 6-hour intervals for 24 hours) into the peritoneal cavity.[25] Thirty minutes after each injection, a cohort of mice was sacrificed, and intestinal sections were stained for BrdU (IHC BrdU kit, Zymed Inc.). The relationship between the ratio of BrdU^{+} cells to PCNA^{+} cells and time was analyzed with a nonlinear mixed effects model, and cell cycle times (*T*) calculated from the slope (*sl*) of the proximal limb of biphasic curves,[25] using the equation: $sl = 1/T$.

For cell migration, three mice per group were sacrificed at 2, 24, and 48 hours after a single intraperitoneal BrdU injection (15 mg/kg), and resulting intestinal sections were subjected to BrdU IHC. Migration rate (μm/hour) reflects the slope of the fitted line of the distance of the farthest labeled enterocyte from the crypt-bottom throughout time. The number (for cell cycle) or the distance (for cell migration) of BrdU-labeled cell(s)/crypt was quantified using NIH Image J software.

Immunoblot Analyses

Epithelia were dissected from normal intestinal mucosa from five individual animals in each group or NCM460 cells (~1,000,000/well in a six-well plate) were synchronized (48 hours) by serum starvation and restimulated with serum alone (control) or that containing 1 mmol/L 8br-cGMP for 3 hours. In each case, protein was extracted in Laemmli buffer containing protease and phosphatase inhibitor cocktails (Pierce, Rockford, IL) and stored at −20°C. Homogenized proteins were subjected to immunoblot analyses using antibodies to the following antigens where indicated: cyclin D1 and pRb from Santa Cruz Biotechnology (1:200 dilution) and cleaved caspase

3 and GAPDH from Cell Signaling (Danvers, MA; 1:1000 dilution). ITF (1:10,000) anti-serum was a gift from Dr. Daniel K. Podolsky (Massachusetts General Hospital and Harvard Medical School, Boston, MA). Bovine anti-goat and anti-rabbit secondary antibodies were from Santa Cruz Biotechnology (1:5000 dilution). Staining intensity of specific bands quantified by densitometry was normalized to that for GAPDH. Average relative intensity reflects the mean of five individual animals per genotype or three independent experiments with NCM460 cells.

In Vitro *Cell Proliferation and Cell Cycle*

For DNA synthesis, NCM460 cells (~50,000/well in a 96-well plate) were synchronized (48 hours) by serum starvation and restimulated (24 hours) with 10% fetal bovine serum in the presence of the indicated treatments. Cells were labeled by adding, for the last 3 hours of incubations, [*methyl*-^{3}H]thymidine (0.2 μCi/well), and [^{3}H]thymidine incorporation into DNA was quantified.[11,13] Also, growth curves were generated by treating NCM460 cells (~50,000/well in a 24-well plate) in media and determining the DNA or protein content per well. After DNA extraction with ethanol in phenol/chloroform, DNA concentrations were measured by spectrophotometry (260 nm) and cell numbers extrapolated from linear standard curves (data not shown). Conversely, protein concentrations were determined using the BCA protein assay kit (Pierce). Cell doubling times (at the period of exponential growth) and cell cycle distributions by flow cytometry (after serum restimulation of synchronized cells) were calculated as described.[11]

Primary Cultures of Colon Mucosa

Colonic tissues were obtained from patients undergoing surgery under a protocol approved by the institutional review board (control no. 01.0823) as a part of the clinical trial NIH R01 CA75123 (S.A. Waldman, PI). Normal colonic mucosa dissected from the lamina propria were cut into 25-mm^2 sheets and placed onto six-well plates in primary culture media.[26] Colonic mucosal sheets incorporated thymidine into nuclear DNA for >21 hours (data not shown). Thus, after isolation and recovery (4 hours), treatments were performed 15 minutes before addition of [methyl-^{3}H]thymidine (2 μCi/well) for 16 hours. Then, ^{3}H-thymidine incorpo-

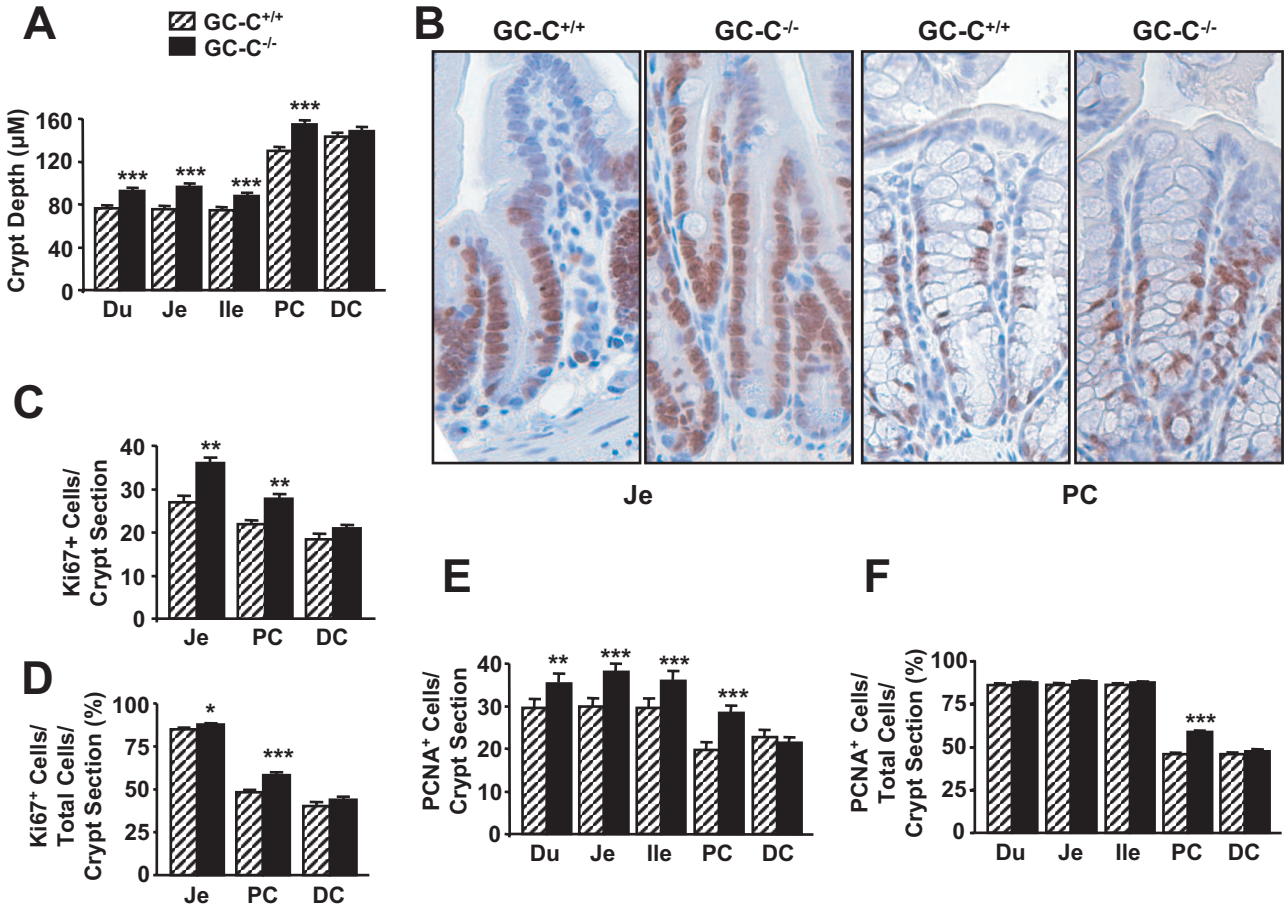

Figure 2. GC-C$^{-/-}$ mice exhibit expanded proliferating compartments. **A:** Crypt depth was increased in GC-C$^{-/-}$ intestinal segments (black columns) compared with their GC-C$^{+/+}$ counterparts (hatched columns). **B:** Ki-67 IHC staining of representative GC-C$^{+/+}$ and GC-C$^{-/-}$ mouse intestinal sections. **C:** Ki-67$^+$ cells per crypt section were increased in GC-C$^{-/-}$ mice. **D:** Ki-67 labeling index (Ki-67$^+$ cell number/total cell number/crypt section) in different intestinal sections. **E:** PCNA$^+$ cells per crypt section were increased in GC-C$^{-/-}$ mice. **F:** PCNA labeling index (PCNA$^+$ cell number/total cell number/crypt section) in different intestinal sections. Du, duodenum; Je, jejunum; Ile, ileum; PC, proximal colon; and DC, distal colon. $^*P < 0.05$, $^{**}P < 0.01$, $^{***}P < 0.0001$ by linear mixed effects model. $n = 9$ mice/genotype. Original magnifications, ×400.

ration into DNA was quantified,[11] and results were normalized to the wet weight of mucosa sheets.

GC-C and Cyclic GMP Analyses

GC-C mRNA was quantified by reverse transcriptase (RT)-PCR.[27] Iodination of ST and GC-C ligand binding was assessed in membranes from NCM460 cells or mouse intestinal mucosa.[23] Specific GC-C binding was calculated using Prism 3.0 software after subtraction of nonspecific binding (with unlabeled ST) from total binding (without unlabeled ST). Finally, cGMP was quantified by radioimmunoassay[28] in NCM460 cells incubated (30 minutes) in serum-free media with the phosphodiesterase inhibitor 3-isobutyl-1-methylxanthine (1 mmol/L) before addition of treatments (for 15 minutes).

Statistics

Crypt depth, cell proliferation by PCNA or Ki-67 IHC, and cell migration were analyzed by fitting a linear mixed effects model.[29] To estimate cell cycle times, a nonlinear mixed effects model[29] was fitted to the crypt-specific proportion ratios of BrdU-labeled cells to $PCNA^+$ cells with the fixed effects part as described.[25] These models accounted for animal-to-animal variability and correlation between clustered measures from the same animal. All other comparisons used the Student's *t*-test. Determinations *in vitro* were repeated at least three times. Where appropriate, analyses were done in triplicate and results reflect mean ± SEM of a representative experiment. In all analyses, $P < 0.05$ was considered statistically significant.

Results

GC-C Regulates the Size of the Proliferating Crypt Compartment

Although the gross histological architecture of crypt and villus units were not obviously different in $GC\text{-}C^{+/+}$ and $GC\text{-}C^{-/-}$ mice (Figure 1H), closer examination revealed that in the absence of GC-C signaling mice exhibited longer crypts (Figure 2A, Table 1; measured with the NIH Image J analysis software) associated with increased numbers of $Ki\text{-}67^+$ (Figure 2, B–D; quantified by $Ki\text{-}67^+$ IHC) or $PCNA^+$ (Figure 2, E and F, and Table 1; quantified by $PCNA^+$ IHC) cells compared with $GC\text{-}C^{+/+}$ mice. Crypt elongation reflected hyperplasia along a decreasing rostral-caudal gradient ($P < 0.001$), and the number of proliferating cells was the dominant predictor of hyperplasia in all intestinal segments ($P < 0.001$). Moreover, the fraction of proliferating cells in crypts (Ki-67- or PCNA-labeling index) increased in $GC\text{-}C^{-/-}$ mice compared with $GC\text{-}C^{+/+}$ mice with the greatest effect in proximal colon (Figure 2, D and F), indicating that crypt hyperplasia principally reflects expansion of the proliferating, and not quiescent, compartment. Indeed, the colonic crypts of Lieberkuhn include the entire cell phenotypic spectrum along the crypt-villus axis, whereas shorter small intestinal crypts (Figure 1H), apically restricted by the crypt-villus junction (Figure 8), are predominantly populated by proliferating progenitor cells (Figure 2B). In agreement with the suggestion that GC-C critically regulates cell proliferative dynamics, induction of GC-C signaling using ST or 8-br-cGMP, a membrane-permeant cGMP analog,[30] inhibited proliferation of normal epithelial cells in mucosal sheets isolated from intestines of patients, as assessed by ^{3}H-thymidine incorporation into nuclear DNA (Figure 3A). Further, ST or the endogenous GC-C agonist guanylin, but not the inactive ST analog TJU 1-103, inhibited proliferation of NCM460 human intestinal crypt cells[22] (Figure 3B), and this effect was mimicked by 8-br-cGMP (Figure 3C).

GC-C Regulates the Rate of the Cell Cycle in the Proliferating Crypt Compartment

To define further the proliferative crypt kinetics in $GC\text{-}C^{-/-}$ mice, cell cycle duration was quantified after serial perito-

Table 1. Crypt Depth and PCNA-Labeled Cell Number

		Crypt depth (μm)			$PCNA^+$ cells/crypt		
			95% Confidence interval			95% Confidence interval	
Genotype	Section	Mean	Lower	Upper	Mean	Lower	Upper
Small intestine							
$GC\text{-}C^{+/+}$	Duodenum	76.2	73.1	79.4	29.5	27.6	31.4
$GC\text{-}C^{-/-}$	Duodenum	92.7*	89.5	95.9	35.4*	33.5	37.3
$GC\text{-}C^{+/+}$	Jejunum	75.0	71.9	78.2	29.9	28.0	31.8
$GC\text{-}C^{-/-}$	Jejunum	96.6*	93.5	99.7	38.1*	36.2	40.0
$GC\text{-}C^{+/+}$	Ileum	74.9	71.8	78.1	29.6	27.7	31.5
$GC\text{-}C^{-/-}$	Ileum	87.4*	84.3	90.5	36.0*	34.2	37.9
Colon							
$GC\text{-}C^{+/+}$	Proximal	129.6	125.6	133.7	19.7	17.9	21.4
$GC\text{-}C^{-/-}$	Proximal	154.3*	150.3	158.3	28.3*	26.5	30.2
$GC\text{-}C^{+/+}$	Distal	142.8	139.2	146.4	22.2	20.3	24.0
$GC\text{-}C^{-/-}$	Distal	146.9	143.2	150.6	20.9	19.1	22.8

Crypt depth and $PCNA^+$ counts reflect analysis of 12 to 106 (median, 47.5) and 4 to 17 (median, 10) crypts/intestinal section/animal. Analyses reflect nine mice for each genotype. *$P \leq 0.0001$, $GC\text{-}C^{-/-}$ versus $GC\text{-}C^{+/+}$.

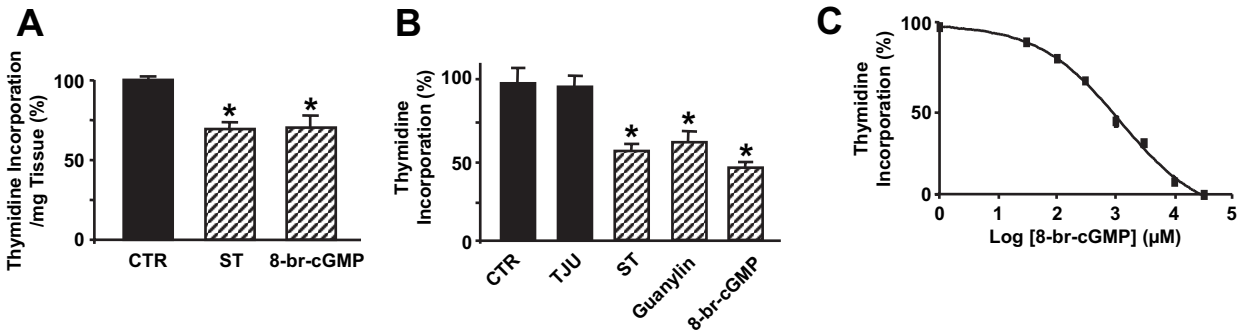

Figure 3. GC-C inhibits proliferation of normal human colonocytes. **A:** DNA synthesis in human colonic mucosa sheets treated with the vehicle (CTR, control), ST (1 μmol/L), or 8-br-cGMP (1 mmol/L). **B:** DNA synthesis in NCM460 cells treated with the vehicle (CTR, control), 1 μmol/L of either the inactive ST analog TJU 1-103 (TJU), ST or guanylin, or 8-br-cGMP (1 mmol/L). Experiments with control, ST, TJU 1-103 or guanylin were performed in the presence of 3-isobutyl-1-methylxanthine (1 mmol/L). **C:** Dose-dependent inhibition of DNA synthesis by 8-br-cGMP in NCM460 cells. Data in **A–C** reflect ^{3}H-thymidine incorporation into nuclear DNA expressed as the percentage of parallel control incubations exposed to the appropriate vehicle. $^*P < 0.05$, two-tailed *t*-test.

neal BrdU injections, with incorporation into DNA by cycling cells during S phase transition (Figure 4A).[25] This model presumes that proliferating crypt cells reflect two populations, including stem cells with a uniform cell cycle that is twice the duration of progenitor cells.[25,31] The nonlinear mixed effects model,[29] used to analyze BrdU labeling curves, was fitted to the crypt-specific proportion ratios of BrdU-labeled cells to PCNA$^+$ cells (Figure 4B). Only cell cycles of progenitor cells were considered, since the model and time (24 hours) used permit quantification of *in vivo* cell

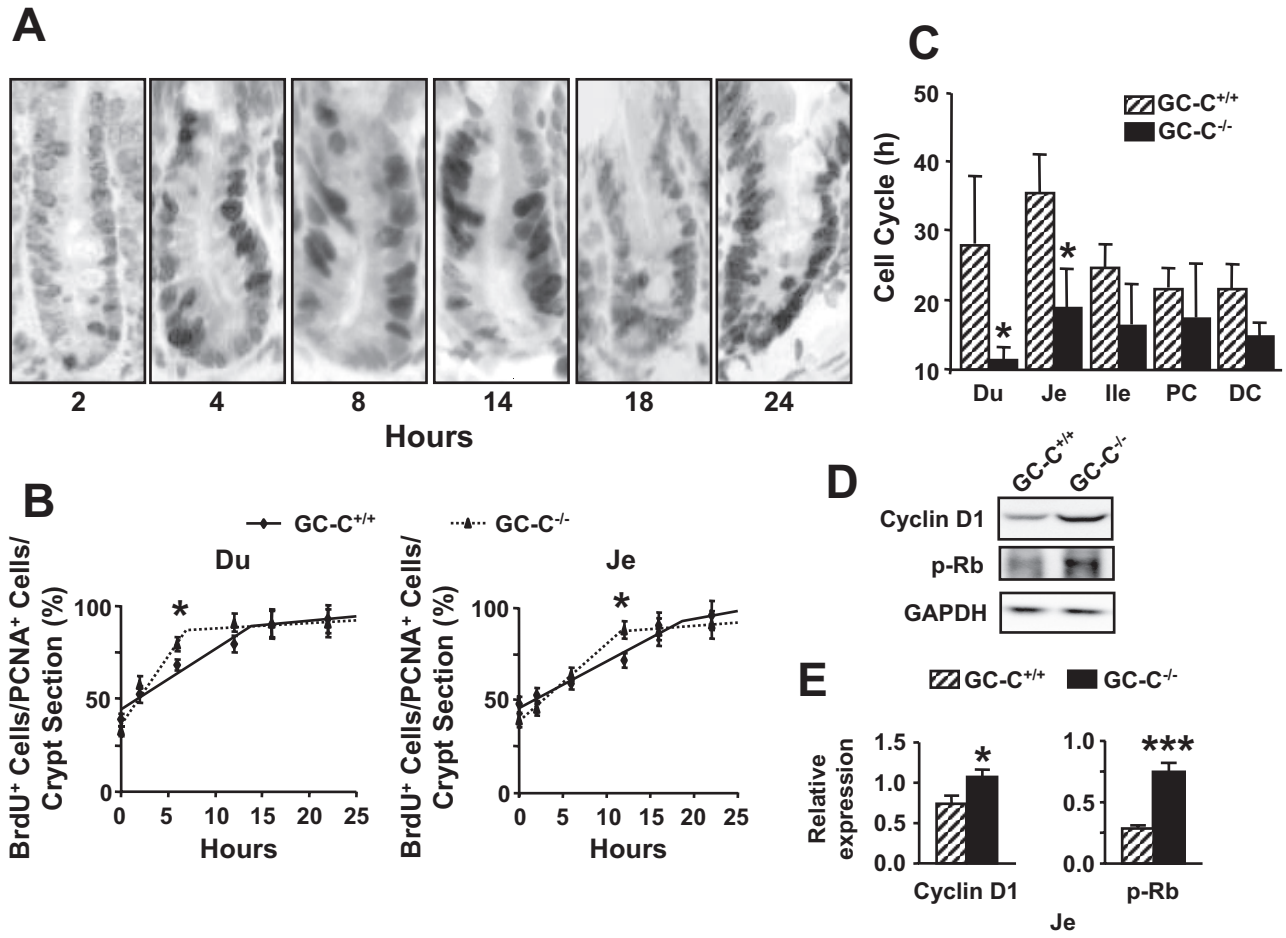

Figure 4. GC-C$^{-/-}$ crypt cells exhibit shorter cell cycles. **A:** Representative BrdU IHC staining of GC-C$^{+/+}$ mouse duodenal slides, after cumulative intraperitoneal injections with BrdU. Proliferating cells are progressively recruited in the BrdU-labeled compartment as a function of their cell cycle time. **B:** BrdU-labeling curves in GC-C$^{-/-}$ (dashed lines) and GC-C$^{+/+}$ (solid lines) mice were generated by calculating the percentage of BrdU-labeled cells per crypt at each time point relative to the average genotype number of PCNA$^+$ cells per crypt in the corresponding intestinal segment. **C:** Cell cycle rates in GC-C$^{-/-}$ (black columns) and GC-C$^{+/+}$ (hatched columns) intestinal segments. **D:** Representative immunoblots of cell cycle mediators cyclin D1 and phosphorylated Rb (p-Rb) in jejunal mucosa from GC-C$^{+/+}$ and GC-C$^{-/-}$ mice. **E:** Mean densitometry of cyclin D1 and p-Rb immunoblots, normalized to GAPDH, from jejunal mucosa of five individual GC-C$^{+/+}$ or GC-C$^{-/-}$ mice, respectively. Intestinal segments are labeled as in Figure 2. **A–C**: $^*P < 0.05$, by linear mixed effects model. **E**: $^*P < 0.05$, $^{**}P < 0.01$, two-tailed *t*-test. Original magnifications, ×400.

Table 2. Cell Cycle Times

Genotype	Section	Cell cycle (hour) Mean	95% Confidence interval Lower	Upper
Small intestine				
GC-C$^{+/+}$	Duodenum	28.3	19.6	37.0
GC-C$^{-/-}$	Duodenum	10.8*	8.1	13.5
GC-C$^{+/+}$	Jejunum	34.1	25.2	43.0
GC-C$^{-/-}$	Jejunum	18.9*	13.6	24.2
GC-C$^{+/+}$	Ileum	24.2	17.5	30.9
GC-C$^{-/-}$	Ileum	17.1	12.4	22.1
Colon				
GC-C$^{+/+}$	Proximal	21.4	17.5	25.2
GC-C$^{-/-}$	Proximal	18.4	11.7	26.1
GC-C$^{+/+}$	Distal	21.8	17.8	25.8
GC-C$^{-/-}$	Distal	15.2	12.5	18.0

*$P < 0.05$, GC-C$^{-/-}$ versus GC-C$^{+/+}$.

cycle rates of rapidly proliferating progenitor cells rather than slowly proliferating stem cells.[3,31] Elimination of GC-C signaling accelerated the cell cycle in crypt progenitor cells of GC-C$^{-/-}$, compared with GC-C$^{+/+}$, mice along a rostrocaudal gradient, with significantly higher effects in proximal small intestine and modest effects in colon (Figure 4, B and C; Table 2). Acceleration of the cell cycle in GC-C$^{-/-}$ mice was associated with increases in critical intestinal cell cycle mediators by immunoblot analysis, including cyclin D1 and p-Rb (Figure 4, D and E).

Conversely, induction of GC-C signaling prolonged the cell cycle of NCM460 human normal colonocytes *in vitro* (Figure 5). Indeed, colonocytes treated with ST (Figure 5A) or 8-br-cGMP (Figure 5B) grew more slowly than control cells receiving PBS, as quantified by the DNA (top panels) or protein (bottom panels) content of cell cultures. Also, intestinal cells exposed to ST (Figure 5C) or 8-br-cGMP (Figure 5D) exhibited a longer doubling time (assessed at the period of exponential growth)[11] associated with a delay in the G_1/S phase transition (Figure 5E). Accordingly, in NCM460 cells cGMP reduced the protein levels of cyclin D1 and p-Rb (Figure 5, F and G), key promoters of the G_1/S cell cycle transition that are regulated by *in vivo* GC-C signaling (Figure 4, D and E).

GC-C-Induced Crypt Hyperplasia Is Coupled with Adaptive Increases in Cell Migration and Apoptosis

Beyond proliferative kinetics, expansion of the crypt progenitor cell compartment in GC-C$^{-/-}$ mice could reflect reduced egress of cells from that compartment, mediated by changes in migration or apoptosis.[2] Proliferating epithelial cells migrated more rapidly along the crypt-villus axis in

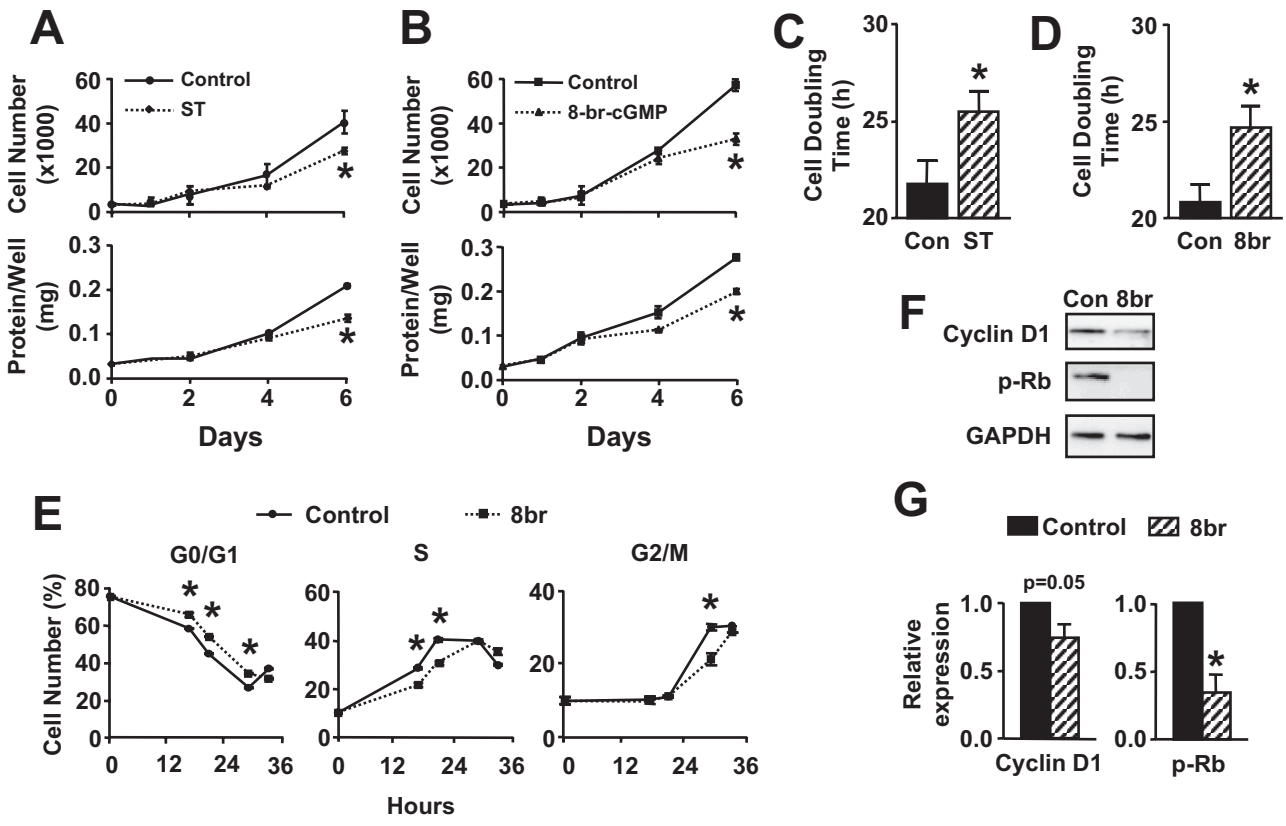

Figure 5. GC-C induces a G_1/S transition delay in normal human colonocytes. Growth curves (**A**, **B**) and cell doubling times (**C**, **D**) of NCM460 cells treated with 1 μmol/L ST (**A**, **C**) or 1 mmol/L 8-br-cGMP (**B**, **D**). **E:** Time course of cell cycle distribution by flow cytometry of NCM460 cells treated with PBS (solid lines) or 1 mmol/L 8-br-cGMP (dashed lines). **F:** Representative immunoblots for cyclin D1 and phosphorylated Rb (p-Rb) in NCM460 cells. **G:** Mean densitometry of cyclin D1 and p-Rb immunoblots, normalized to GAPDH, from three independent experiments. Con, control (cells treated with PBS); 8br, 8-br-cGMP. *$P < 0.05$, two-tailed *t*-test.

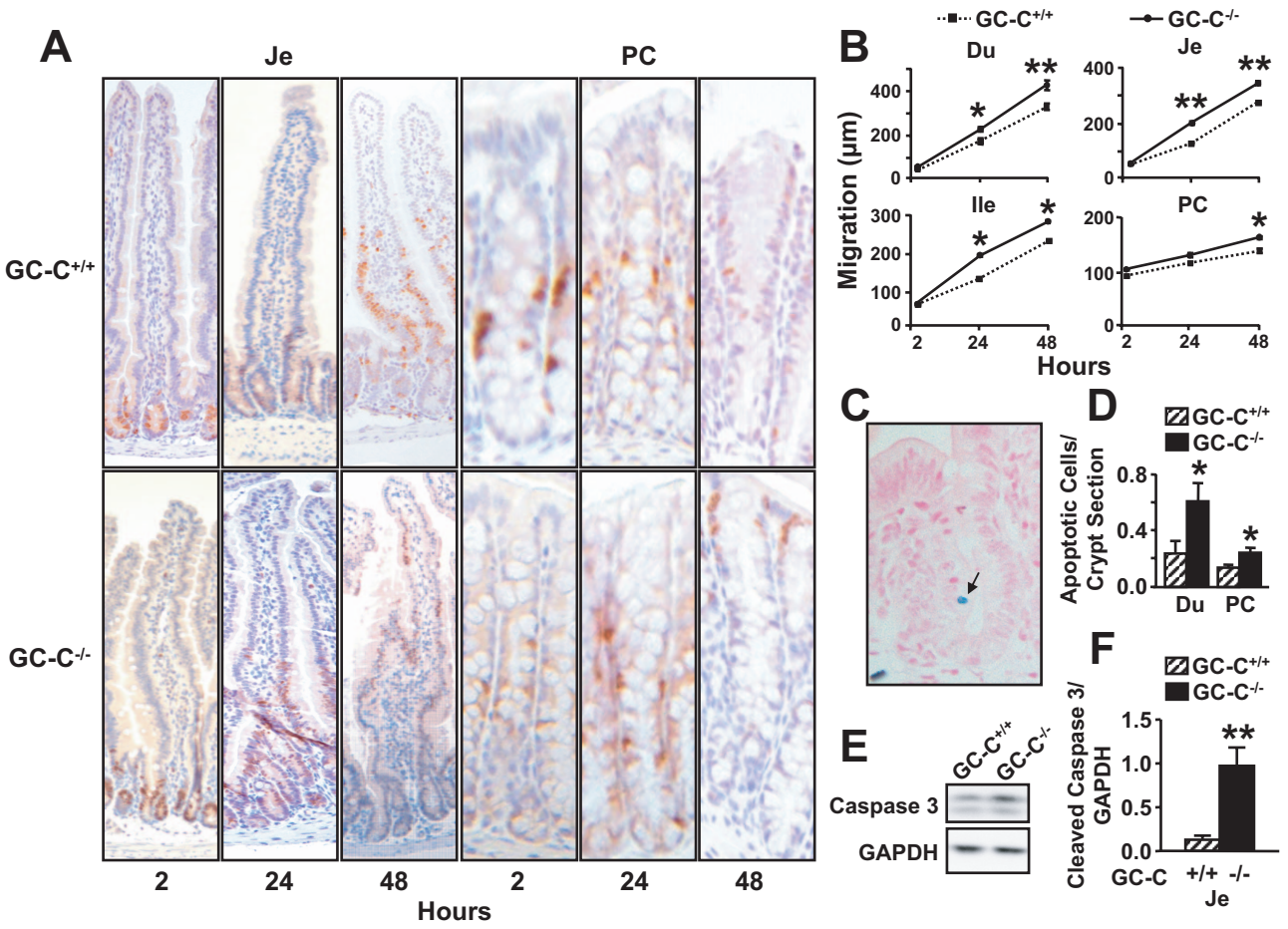

Figure 6. Adaptive increases in migration and apoptosis along the GC-C$^{-/-}$ crypt-villus axis. **A:** BrdU IHC staining of representative intestinal sections from mice receiving a single BrdU injection to quantify cell migration. **B:** Quantification of intestinal epithelial cell migration. **C** and **D:** Apoptosis was quantified by TUNEL staining (**C**) after scoring 100 to 800 crypts/intestinal segment in five GC-C$^{+/+}$ (hatched columns) and five GC-C$^{-/-}$ (black columns) mice (**D**). **E:** Representative immunoblots of cleaved caspase 3 in jejunal mucosa from GC-C$^{+/+}$ and GC-C$^{-/-}$ mice. **F:** Mean densitometry of cleaved caspase 3 immunoblots, normalized to GAPDH, from jejunal mucosa of five individual GC-C$^{+/+}$ or GC-C$^{-/-}$ mice. Intestinal segments are labeled as in Figure 2. *$P < 0.05$; **$P < 0.01$, two-tailed *t*-test. Original magnifications: ×200 (**A**, jejunum); × 400 (**A**, proximal colon; **C**).

GC-C$^{-/-}$ compared with GC-C$^{+/+}$ mice (Figure 6, A and B, and Table 3; quantified by single intraperitoneal BrdU injection). Linear mixed effects modeling, which considered animal-average scores of PCNA^{+} cells and crypt depth, suggests that accelerated enterocyte migration was an adaptive response to, rather than the cause of, crypt hyper-

Table 3. Cell Migration Rates

		Crypt migration (μm/hour)			Δ Migration [(GC-C$^{-/-}$) − GC-C$^{+/+}$]		
			95% Confidence interval			95% Confidence interval	
Genotype	Section	Mean	Lower	Upper	Mean	Lower	Upper
Small intestine							
GC-C$^{+/+}$	Duodenum	23.3	21.1	25.4			
GC-C$^{-/-}$	Duodenum	31.8*	29.7	33.9	8.5	5.6	11.5
GC-C$^{+/+}$	Jejunum	19.6	17.5	21.7			
GC-C$^{-/-}$	Jejunum	24.1†	22.0	26.2	4.5	1.6	7.4
GC-C$^{+/+}$	Ileum	15.2	13.2	17.2			
GC-C$^{-/-}$	Ileum	18.4‡	16.4	20.5	3.3	0.4	6.1
Colon							
GC-C$^{+/+}$	Proximal	3.9	1.9	6.0			
GC-C$^{-/-}$	Proximal	4.4	2.4	6.5	0.5	−2.4	3.3
GC-C$^{+/+}$	Distal	3.6	1.6	5.5			
GC-C$^{-/-}$	Distal	1.3	−0.7	3.4	−2.3	−5.1	0.6

Migration distances traveled by enterocytes were measured in 2 to 72 (median, 24) crypts/intestinal section/animal.
*$P < 0.0001$, $^{\dagger}P < 0.01$, $^{\ddagger}P < 0.05$, GC-C$^{-/-}$ versus GC-C$^{+/+}$.

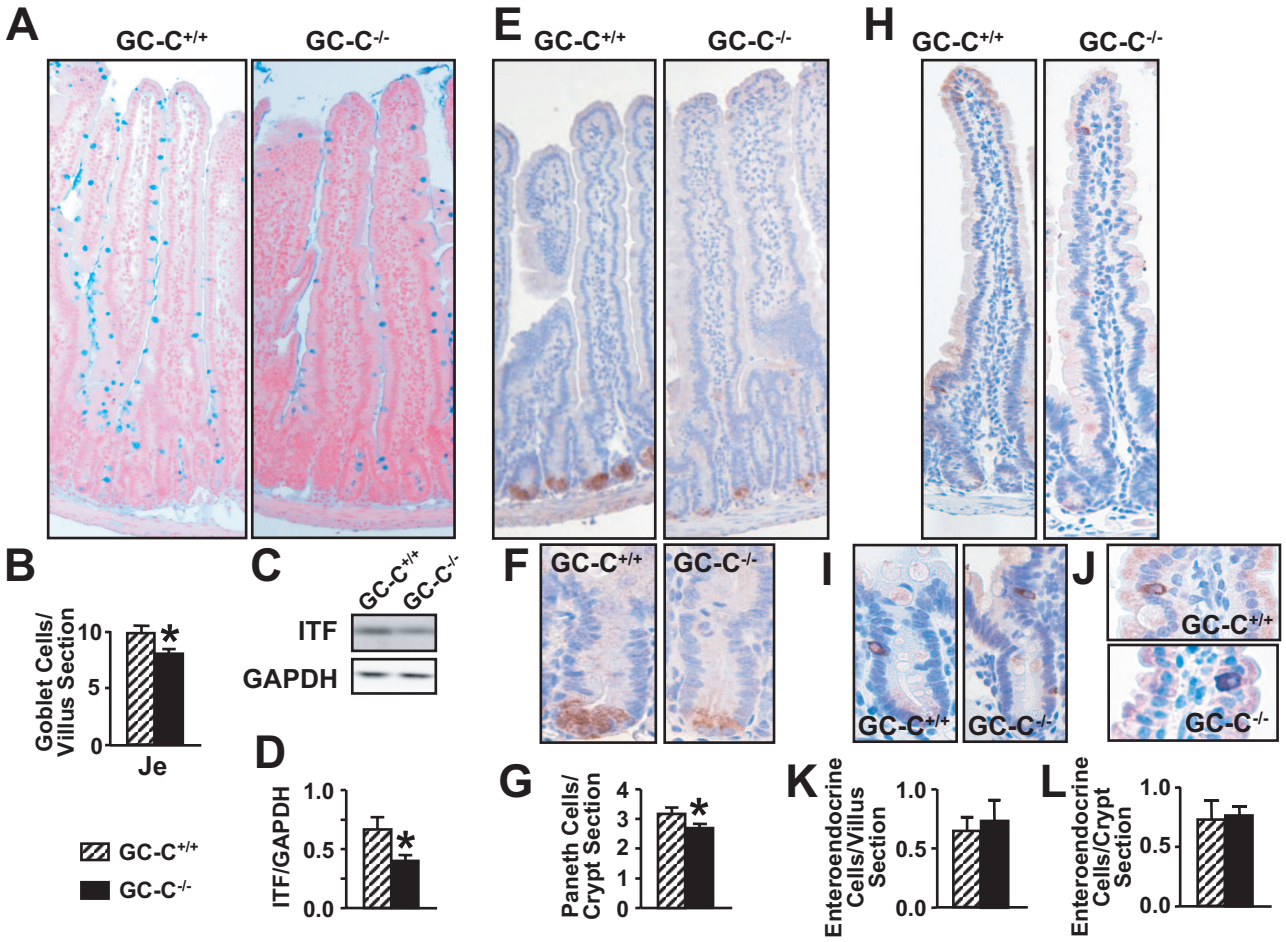

Figure 7. Lineage-specific cell commitment is altered in GC-C$^{-/-}$ mice. **A–D:** Goblet cells were detected by Alcian blue staining (**A**) and enumerated in 3 to 15 villi per mouse (**B**). Expression of intestinal trefoil factor (ITF), a goblet cell marker, was detected by immunoblot analysis (**C**) and quantified by average densitometry, after normalization to GAPDH, in colons from five individual GC-C$^{+/+}$ and GC-C$^{-/-}$ mice, respectively (**D**). **E–G:** Paneth cells (**E**, **F**) were detected by lysozyme staining and enumerated in ~10 crypts per mouse (**G**). **H–L:** Enteroendocrine cells (**H**, **I,** crypts; **J,** villi) were quantified in ~100 crypts per mouse (**K**) or ~20 villi per mouse (**L**) by chromogranin A staining. Data in **B**, **D**, **G**, **K**, and **L** reflect analysis of jejunal (Je) sections from nine GC-C$^{+/+}$ (hatched columns) or nine GC-C$^{-/-}$ (black columns) mice, respectively. *$P < 0.05$, two-tailed *t*-test. Original magnifications: ×200 (**A**, **E**, **H**); ×400 (**F**, **I**, **J**).

plasia ($P < 0.001$). Indeed, as observed for proliferative kinetics, GC-C-dependent regulation of cell migration exhibited a rostro-caudal gradient (Table 3). Similarly, elimination of GC-C increased apoptosis in intestinal crypts as assessed by TUNEL (Figure 6, C and D) and immunoblot analysis for cleaved caspase 3 (Figure 6, E and F), also reflecting an adaptive response to crypt hyperplasia.

GC-C Regulates Lineage-Specific Cell Differentiation

Perturbations in cell maturation dynamics also could contribute to the expansion of crypt compartments in GC-C$^{-/-}$ mice.[2] Indeed, elimination of GC-C signaling specifically altered cell-lineage differentiation, and GC-C$^{-/-}$ mice exhibited fewer goblet cells compared with wild-type mice, as assessed by counting intestinal cells stained for mucin with Alcian blue (Figure 7, A and B) and by immunoblot analysis for intestine trefoil factor (Figure 7, C and D). In addition, GC-C$^{-/-}$ mice exhibited fewer Paneth cells than GC-C$^{+/+}$ mice, as quantified by counting mucosal cells stained with anti-lysozyme antibody (Figure 7, E–G). However, there were no differences in enteroendocrine cells (Figure 7, H–L; quantified by IHC for anti-chromogranin A) or absorptive enterocytes (Figure 8; quantified by IHC for villin). Further, the ordered transition from the proliferating (Ki-67^{+}) to the differentiated (villin^{+}) cell compartment was maintained in GC-C$^{-/-}$ mice (Figure 8). Moreover, there were no differences in villus length in GC-C$^{-/-}$, compared with GC-C$^{+/+}$, mice (data not shown). Taken together, these data suggest that GC-C signaling critically affects the homeostasis of intestinal crypt compartment by coordinating processes underlying reciprocal regulation of proliferation and differentiation associated with adaptive responses in migration and apoptosis.

Discussion

The importance of defining the molecular mechanisms organizing the crypt-villus axis is underscored by the established relationship between dysregulation of key processes underlying that organization and intestinal tu-

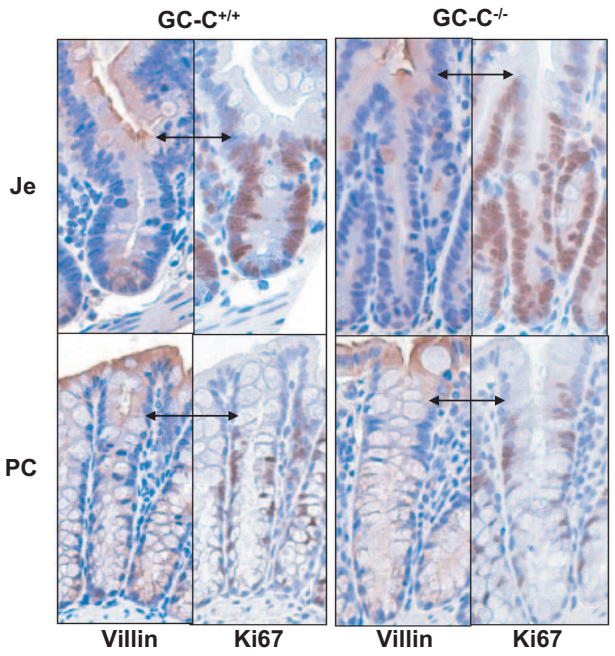

Figure 8. The transition from proliferating to differentiated absorptive cells is retained in GC-C$^{-/-}$ mice. IHC staining of representative small (jejunum, Je) and large (proximal colon, PC) intestinal sections from GC-C$^{+/+}$ and GC-C$^{-/-}$ mice. Mature enterocytes and proliferating crypt cells were visualized in adjacent sections after staining for villin and Ki-67, respectively. **Double-headed arrows** indicate the cell position of the transition from proliferation to enterocyte differentiation (first villin^{+}/Ki-67^{-} cell from the crypt bottom). Original magnifications, ×400.

morigenesis.[4,6,8] Thus, Wnt/β-catenin/Tcf-4 pathway is a principal determinant of the crypt cell phenotype,[32] and mice with disrupted Tcf-4 signaling exhibit depletion of intestinal stem cell compartments.[33] Ca^{2+} inhibits proliferation and promotes differentiation in intestinal mucosa,[34] and Ca^{2+} supplementation abrogated intestinal hyperproliferation and tumor formation in *Apc*$^{Min/+}$ mice.[35] Further, CDX-2 is a transcription factor of the murine homeobox gene family that regulates intestinal epithelial cell differentiation[36] and its reduced expression was associated with colon tumorigenesis in *Apc*$^{Min/+}$ mice.[37]

In that context, GC-C signaling has emerged as a key modulator of the colon cancer cell phenotype. GC-C inhibits colon cancer cell proliferation[11–13] and opposes colon carcinogenesis in *Apc*$^{Min/+}$ mice.[14,38] Also, although GC-C expression is highly conserved,[23] expression of guanylin and uroguanylin is uniformly lost early in neoplastic transformation, suggesting that disruption of GC-C signaling may contribute to colon carcinogenesis.[14,19] GC-C and cGMP inhibit tumor cell proliferation by inducing Ca^{2+} influx through cyclic nucleotide gated channels,[12] suggesting that the anti-tumor effects of dietary Ca^{2+} [34,35] may be mediated, in part, by GC-C signaling. Moreover, activation of GC-C may oppose pro-proliferative Wnt/β-catenin/Tcf-4 signaling by promoting PKG1β-dependent degradation of β-catenin, inhibiting its nuclear translocation.[39]

Beyond colon cancer cell proliferation, the role of GC-C in mechanisms underlying normal intestinal epithelial cell dynamics remains undefined. Elimination of guanylin expression in mice produced colonic crypt hyperplasia, reflecting expansion of proliferative compartments associated with increased migration.[20] Although reminiscent of observations in the present study, these effects were not replicated in GC-C$^{-/-}$ mice,[21] suggesting that other receptors mediate the effects of guanylin on colon crypt dynamics. Indeed, receptors other than GC-C may mediate effects of GC-C ligands on fluid homeostasis.[40] However, previous studies examining crypt dynamics in GC-C$^{-/-}$ mice did not present data and did not specify the anatomical segment along the rostro-caudal axis analyzed.[21] As demonstrated herein, experimental measurements confined to the distal colon in GC-C$^{-/-}$ mice could have produced artifactually negative results.

Here, elimination of GC-C induced selective crypt hyperplasia along a decreasing rostro-caudal gradient, in the absence of changes in villus morphology. Crypt hyperplasia reflected, in part, increases in the number of proliferating cells and acceleration of their cell cycle. These changes were associated with adaptive increases in migration and apoptosis along the crypt-villus axis, which limited expansion of the proliferating compartment. Thus, GC-C signaling represents a previously unrecognized mechanism restricting the size and proliferative rate of the intestinal progenitor compartment. The rostral-caudal gradient of this effect likely reflects a recapitulation of the established gradient along that axis of proliferation, migration, and apoptosis[41,42] and the quantitative and qualitative differences in downstream effector mechanisms mediating GC-C signaling.[20,43–46] In the context of the present studies, crypt elongation associated with increases in proliferation and migration previously observed in guanylin$^{-/-}$ mice reflect elimination of GC-C signaling, rather than loss of signaling by another unidentified receptor.[20]

The present study reveals a previously unappreciated role for GC-C in mechanisms regulating proliferative indices of normal intestinal epithelial cells. Indeed, GC-C signaling inhibited DNA synthesis rates in normal colonocytes in human mucosa sheets and in human intestinal epithelial cells. Moreover, GC-C signaling prolonged the intestinal epithelial cell cycle by inducing a G_1/S delay. Crypt hyperplasia associated with increased numbers of rapidly cycling progenitor cells in GC-C$^{-/-}$ mice reflects loss of physiological GC-C regulation of the cell cycle. In contrast, GC-C-induced cytostasis in colon cancer cells reflects a generalized slowing, without delay in any specific phase, of the cell cycle.[11–13] In that context, GC-C-induced G_1/S delay may represent a novel tumor-suppressor mechanism in normal cells whose interruption, through loss of ligand expression,[17–19] contributes to colon tumorigenesis.

In addition, this study reveals a role for GC-C signaling in lineage-specific maturation of intestinal epithelial cells. In GC-C$^{-/-}$ mice, crypt hyperplasia reflected increases in proliferative dynamics and reciprocal restriction of differentiation along the secretory lineage, specifically of Paneth and goblet cells, without effects on enteroendocrine cells or absorptive enterocytes. The selective impairment of cell lineage commitment suggests that, rather than a passive consequence of dysregulated cell proliferation, these ef-

fects may reflect a previously unrecognized ability of GC-C to regulate discreet molecular mechanisms associated with intestinal cell programming.

Beyond fluid balance, GC-C has recently emerged as a critical signaling molecule suppressing colorectal tumorigenesis by regulating distinct, mutually reinforcing molecular mechanisms underlying crypt-villus homeostasis, including restriction of proliferation and maintenance of genomic integrity.[38] Observations presented here further support the suggestion that GC-C is one of the integrated paracrine mechanisms regulating intestinal mucosa homeostasis. Thus, GC-C signaling restricts the size of crypt progenitor compartments, impeding cell cycle progression and proliferation, promoting lineage-specific maturation, limiting cell migration, and inhibiting apoptosis. The pathophysiological significance of GC-C as a paracrine mechanism restricting the size of the proliferating compartment is underscored by the centrality of this compartment in mechanisms underlying colon carcinogenesis. Indeed, overexpression of molecules like Wnt, β-catenin, and Tcf that promote the progenitor cell compartment in the crypt is associated with colonic tumorigenesis.[32,33] Conversely, disruption of genes including *APC*, *SMAD*, and *IHH*, which restrict the proliferating crypt compartment and promote differentiation in the villus compartment, also is associated with colonic tumorigenesis.[47–51] The prevailing model suggests that tumor initiation and progression in colon reflects accumulation of genetic mutations in proliferating crypt progenitor cells.[52] Importantly, expression of guanylin and uroguanylin is invariably lost early during neoplastic transformation.[17–19] In the context of the present studies, early loss of GC-C ligands and the associated physiological mechanisms restricting the cell cycle, number of proliferating cells and size of the progenitor compartment, and promoting cell differentiation will induce crypt hyperplasia, amplifying accumulation of stochastic genetic mutations underlying tumor initiation.[4,6,8] Moreover, dysregulated GC-C signaling reflecting loss of ligands eliminates one important cytostatic mechanism inhibiting proliferation in transformed cells, potentiating tumor promotion.[11–13,30] Of significance, loss of guanylin and uroguanylin expression in human tumors is associated with near-uniform overexpression of GC-C,[23,27] suggesting paracrine hormone replacement therapy as a novel chemopreventive strategy to maintain crypt-villus homeostasis and suppress tumor initiation and promotion in intestine.[38]

References

1. Nordgaard I, Mortensen PB: Digestive processes in the human colon. Nutrition 1995, 11:37–45
2. Potten CS, Loeffler M: Stem cells: attributes, cycles, spirals, pitfalls and uncertainties. Lessons for and from the crypt. Development 1990, 110:1001–1020
3. Bach SP, Renehan AG, Potten CS: Stem cells: the intestinal stem cell as a paradigm. Carcinogenesis 2000, 21:469–476
4. Montgomery RK, Mulberg AE, Grand RJ: Development of the human gastrointestinal tract: twenty years of progress. Gastroenterology 1999, 116:702–731
5. Jemal A, Tiwari RC, Murray T, Ghafoor A, Samuels A, Ward E, Feuer EJ, Thun MJ: Cancer statistics, 2004. CA Cancer J Clin 2004, 54:8–29
6. Yang WC, Mathew J, Velcich A, Edelmann W, Kucherlapati R, Lipkin M, Yang K, Augenlicht LH: Targeted inactivation of the p21(WAF1/cip1) gene enhances Apc-initiated tumor formation and the tumor-promoting activity of a Western-style high-risk diet by altering cell maturation in the intestinal mucosal. Cancer Res 2001, 61:565–569
7. Velcich A, Yang W, Heyer J, Fragale A, Nicholas C, Viani S, Kucherlapati R, Lipkin M, Yang K, Augenlicht L: Colorectal cancer in mice genetically deficient in the mucin Muc2. Science 2002, 295:1726–1729
8. Sakatani T, Kaneda A, Iacobuzio-Donahue CA, Carter MG, de Boom Witzel S, Okano H, Ko MS, Ohlsson R, Longo DL, Feinberg AP: Loss of imprinting of Igf2 alters intestinal maturation and tumorigenesis in mice. Science 2005, 307:1976–1978
9. Lucas KA, Pitari GM, Kazerounian S, Ruiz-Stewart I, Park J, Schulz S, Chepenik KP, Waldman SA: Guanylyl cyclases and signaling by cyclic GMP. Pharmacol Rev 2000, 52:375–414
10. Vaandrager AB, Bot AG, De Vente J, De Jonge HR: Atriopeptins and Escherichia coli enterotoxin STa have different sites of action in mammalian intestine. Gastroenterology 1992, 102:1161–1169
11. Pitari GM, Di Guglielmo MD, Park J, Schulz S, Waldman SA: Guanylyl cyclase C agonists regulate progression through the cell cycle of human colon carcinoma cells. Proc Natl Acad Sci USA 2001, 98:7846–7851
12. Pitari GM, Zingman LV, Hodgson DM, Alekseev AE, Kazerounian S, Bienengraeber M, Hajnoczky G, Terzic A, Waldman SA: Bacterial enterotoxins are associated with resistance to colon cancer. Proc Natl Acad Sci USA 2003, 100:2695–2699
13. Pitari GM, Baksh RI, Harris DM, Li P, Kazerounian S, Waldman SA: Interruption of homologous desensitization in cyclic guanosine 3′,5′-monophosphate signaling restores colon cancer cytostasis by bacterial enterotoxins. Cancer Res 2005, 65:11129–11135
14. Shailubhai K, Yu HH, Karunanandaa K, Wang JY, Eber SL, Wang Y, Joo NS, Kim HD, Miedema BW, Abbas SZ, Boddupalli SS, Currie MG, Forte LR: Uroguanylin treatment suppresses polyp formation in the Apc(Min/+) mouse and induces apoptosis in human colon adenocarcinoma cells via cyclic GMP. Cancer Res 2000, 60:5151–5157
15. Pilz RB, Casteel DE: Regulation of gene expression by cyclic GMP. Circ Res 2003, 93:1034–1046
16. Hewitson TD, Martic M, Darby IA, Kelynack KJ, Bisucci T, Tait MG, Becker GJ: Intracellular cyclic nucleotide analogues inhibit in vitro mitogenesis and activation of fibroblasts derived from obstructed rat kidneys. Nephron Exp Nephrol 2004, 96:59–66
17. Zhang L, Zhou W, Velculescu VE, Kern SE, Hruban RH, Hamilton SR, Vogelstein B, Kinzler KW: Gene expression profiles in normal and cancer cells. Science 1997, 276:1268–1272
18. Steinbrecher KA, Tuohy TM, Heppner Goss K, Scott MC, Witte DP, Groden J, Cohen MB: Expression of guanylin is downregulated in mouse and human intestinal adenomas. Biochem Biophys Res Commun 2000, 273:225–230
19. Notterman DA, Alon U, Sierk AJ, Levine AJ: Transcriptional gene expression profiles of colorectal adenoma, adenocarcinoma, and normal tissue examined by oligonucleotide arrays. Cancer Res 2001, 61:3124–3130
20. Steinbrecher KA, Wowk SA, Rudolph JA, Witte DP, Cohen MB: Targeted inactivation of the mouse guanylin gene results in altered dynamics of colonic epithelial proliferation. Am J Pathol 2002, 161:2169–2178
21. Mann EA, Steinbrecher KA, Stroup C, Witte DP, Cohen MB, Giannella RA: Lack of guanylyl cyclase C, the receptor for Escherichia coli heat-stable enterotoxin, results in reduced polyp formation and increased apoptosis in the multiple intestinal neoplasia (Min) mouse model. Int J Cancer 2005, 116:500–505
22. Moyer MP, Manzano LA, Merriman RL, Stauffer JS, Tanzer LR: NCM460, a normal human colon mucosal epithelial cell line. In Vitro Cell Dev Biol Anim 1996, 32:315–317
23. Carrithers SL, Barber MT, Biswas S, Parkinson SJ, Park PK, Goldstein SD, Waldman SA: Guanylyl cyclase C is a selective marker for metastatic colorectal tumors in human extraintestinal tissues. Proc Natl Acad Sci USA 1996, 93:14827–14832
24. Schulz S, Lopez MJ, Kuhn M, Garbers DL: Disruption of the guanylyl cyclase-C gene leads to a paradoxical phenotype of viable but

heat-stable enterotoxin-resistant mice. J Clin Invest 1997, 100: 1590–1595
25. Nowakowski RS, Lewin SB, Miller MW: Bromodeoxyuridine immunohistochemical determination of the lengths of the cell cycle and the DNA-synthetic phase for an anatomically defined population. J Neurocytol 1989, 18:311–318
26. Birkner S, Weber S, Dohle A, Schmahl G, Follmann W: Growth and characterisation of primary bovine colon epithelial cells in vitro. Altern Lab Anim 2004, 32:555–571
27. Schulz S, Hyslop T, Haaf J, Bonaccorso C, Nielsen K, Witek ME, Birbe R, Palazzo J, Weinberg D, Waldman SA: A validated quantitative assay to detect occult micrometastases by reverse transcriptase-polymerase chain reaction of guanylyl cyclase C in patients with colorectal cancer. Clin Cancer Res 2006, 12:4545–4552
28. Kazerounian S, Pitari GM, Shah FJ, Frick GS, Madesh M, Ruiz-Stewart I, Schulz S, Hajnoczky G, Waldman SA: Proliferative signaling by store-operated calcium channels opposes colon cancer cell cytostasis induced by bacterial enterotoxins. J Pharmacol Exp Ther 2005, 314:1013–1022
29. Vonesh EF, Chinchilli VM: Linear and Nonlinear Models for the Analysis of Repeated Measures. New York, Marcel Dekker, 1997
30. Pitari GM, Li T, Baksh RI, Waldman SA: Exisulind and guanylyl cyclase C induce distinct antineoplastic signaling mechanisms in human colon cancer cells. Mol Cancer Ther 2006, 5:1190–1196
31. Potten CS: Cell cycles in cell hierarchies. Int J Radiat Biol Relat Stud Phys Chem Med 1986, 49:257–278
32. Gregorieff A, Clevers H: Wnt signaling in the intestinal epithelium: from endoderm to cancer. Genes Dev 2005, 19:877–890
33. Korinek V, Barker N, Moerer P, van Donselaar E, Huls G, Peters PJ, Clevers H: Depletion of epithelial stem-cell compartments in the small intestine of mice lacking Tcf-4. Nat Genet 1998, 19:379–383
34. Whitfield JF, Bird RP, Chakravarthy BR, Isaacs RJ, Morley P: Calcium-cell cycle regulator, differentiator, killer, chemopreventor, and maybe, tumor promoter. J Cell Biochem Suppl 1995, 22:S74–S91
35. Newmark HL, Yang K, Lipkin M, Kopelovich L, Liu Y, Fan K, Shinozaki H: A Western-style diet induces benign and malignant neoplasms in the colon of normal C57Bl/6 mice. Carcinogenesis 2001, 22: 1871–1875
36. Freund JN, Domon-Dell C, Kedinger M, Duluc I: The Cdx-1 and Cdx-2 homeobox genes in the intestine. Biochem Cell Biol 1998, 76:957–969
37. Aoki K, Tamai Y, Horiike S, Oshima M, Taketo MM: Colonic polyposis caused by mTOR-mediated chromosomal instability in Apc+/Delta716 Cdx2+/− compound mutant mice. Nat Genet 2003, 35:323–330
38. Li P, Schulz S, Bombonati A, Palazzo JP, Hyslop TM, Barab AA, Siracusa LD, Pitari GM, Waldman SA: Guanylyl cyclase C suppresses intestinal tumorigenesis by restricting proliferation and maintaining genomic integrity. Gastroenterology 2007, 133:599–607
39. Thompson WJ, Piazza GA, Li H, Liu L, Fetter J, Zhu B, Sperl G, Ahnen D, Pamukcu R: Exisulind induction of apoptosis involves guanosine 3′,5′-cyclic monophosphate phosphodiesterase inhibition, protein kinase G activation, and attenuated beta-catenin. Cancer Res 2000, 60:3338–3342
40. Sindić A, Velic A, Basoglu C, Hirsch JR, Edemir B, Kuhn M, Schlatter E: Uroguanylin and guanylin regulate transport of mouse cortical collecting duct independent of guanylate cyclase C. Kidney Int 2005, 68:1008–1017
41. Marshman E, Booth C, Potten CS: The intestinal epithelial stem cell. Bioessays 2002, 24:91–98
42. Potten CS: Keratinocyte stem cells, label-retaining cells and possible genome protection mechanisms. J Invest Dermatol Symp Proc 2004, 9:183–195
43. Vaandrager AB, Bot AG, De Jonge HR: Guanosine 3′,5′-cyclic monophosphate-dependent protein kinase II mediates heat-stable enterotoxin-provoked chloride secretion in rat intestine. Gastroenterology 1997, 112:437–443
44. Forte LR, Thorne PK, Eber SL, Krause WJ, Freeman RH, Francis SH, Corbin JD: Stimulation of intestinal Cl− transport by heat-stable enterotoxin: activation of cAMP-dependent protein kinase by cGMP. Am J Physiol 1992, 263:C607–C615
45. Chao AC, de Sauvage FJ, Dong YJ, Wagner JA, Goeddel DV, Gardner P: Activation of intestinal CFTR Cl− channel by heat-stable enterotoxin and guanylin via cAMP-dependent protein kinase. EMBO J 1994, 13:1065–1072
46. Vaandrager AB, Bot AG, Ruth P, Pfeifer A, Hofmann F, De Jonge HR: Differential role of cyclic GMP-dependent protein kinase II in ion transport in murine small intestine and colon. Gastroenterology 2000, 118:108–114
47. van den Brink GR, Hardwick JC, Tytgat GN, Brink MA, Ten Kate FJ, Van Deventer SJ, Peppelenbosch MP: Sonic hedgehog regulates gastric gland morphogenesis in man and mouse. Gastroenterology 2001, 121:317–328
48. van den Brink GR, Bleuming SA, Hardwick JC, Schepman BL, Offerhaus GJ, Keller JJ, Nielsen C, Gaffield W, van Deventer SJ, Roberts DJ, Peppelenbosch MP: Indian Hedgehog is an antagonist of Wnt signaling in colonic epithelial cell differentiation. Nat Genet 2004, 36:277–282
49. Tang Y, Katuri V, Srinivasan R, Fogt F, Redman R, Anand G, Said A, Fishbein T, Zasloff M, Reddy EP, Mishra B, Mishra L: Transforming growth factor-beta suppresses nonmetastatic colon cancer through Samd4 and adaptor protein Elf at an early stage of tumorigenesis. Cancer Res 2005, 65:4228–4237
50. Takaku K, Oshima M, Miyoshi H, Matsui M, Seldin MF, Taketo MM: Intestinal tumorigenesis in compound mutant mice of both Dpc4 (Smad4) and Apc genes. Cell 1998, 92:645–656
51. Fodde R, Kuipers J, Rosenberg C, Smits R, Kielman M, Gaspar C, van Es JH, Breukel C, Wiegant J, Giles RH, Clevers H: Mutations in the APC tumour suppressor gene cause chromosomal instability. Nat Cell Biol 2001, 3:433–438
52. Radtke F, Clevers H: Self-renewal and cancer of the gut: two sides of a coin. Science 2005, 307:1904–1909